Applied Energy 93 (2012) 33–38

Contents lists available at ScienceDirect

Applied Energy

journal homepage: www.elsevier.com/locate/apenergy

Thermal design and management for performance optimization of solar thermoelectric generator

Jinsheng Xiao [a,b,*], Tianqi Yang [a], Peng Li [b], Pengcheng Zhai [b], Qingjie Zhang [b]

[a] School of Automotive Engineering, Wuhan University of Technology, Hubei 430070, China
[b] State Key Laboratory of Advanced Technology for Materials Synthesis and Processing, Wuhan University of Technology, Hubei 430070, China

ARTICLE INFO

Article history:
Received 30 October 2010
Received in revised form 16 May 2011
Accepted 1 June 2011
Available online 2 July 2011

Keywords:
Solar energy
Thermoelectric module
Thermoelectric generator
Performance optimization
Finite element analysis

ABSTRACT

We established a three-dimensional finite element model of thermoelectric module based on low-temperature thermoelectric material bismuth telluride and medium-temperature thermoelectric material filled-skutterudite. The material properties of the thermoelectric materials such as the Seebeck coefficient, thermal conductivity, and electrical conductivity are temperature dependent. Based on the formal model, multi-stage models consist of low- and medium-temperature thermoelectric modules are proposed. The effect of input energy on performance of solar thermoelectric generator is considered according to the real operating condition. Results show that, reasonable thermal design of solar thermoelectric generator can take full advantage of the characteristics of thermoelectric materials and effectively improve the performance of power generation.

1. Introduction

Solar thermoelectric generator, which uses concentrated solar radiation as heat source, has been studied for many years. Chen developed a thermodynamic model for discussing the performance of solar-driven thermoelectric generator [1]. Scherrer et al. developed a numerical model of solar thermoelectric generator base on skutterudite for satellite [2]. Omer and Infield presented an improved theoretical model of solar thermoelectric generator which includes all parameters that have an influence on the heat transfer process, and the modeling results are compared with experimental data of the commercial thermoelectric module in power generation mode [3]. Li et al. presented a prototype concentration solar thermoelectric generator (CTG) and a discrete numerical model for the evaluation of the whole system [4]. All these theoretical and experimental studies lay a foundation for the development of solar thermoelectric generator.

There are many advantages of solar thermoelectric generator, such as endless shelf life, simple structure, no moving parts, silent in operation and no pollution. However, the low conversion efficiency makes it hard to be widely used. The conversion efficiency of solar thermoelectric generator is mainly restricted by thermoelectric materials. Over the past several years, a number of high performance thermoelectric materials have been developed [5,6], and some of them are available commercially. Bismuth telluride is a favorable low-temperature thermoelectric material, which exerts better property at low temperature (25–225 °C) [7,8]. While filled-skutterudite is a good medium-temperature thermoelectric material, that can be used for wide temperature range generation (25–525 °C) [9].

In addition to the research of thermoelectric materials, reasonable thermal design and management of thermoelectric generator is equally important for improving the generating performance. Chen et al. established a theoretical model of a two-stage semiconductor thermoelectric generator [10]. El-Genk and Saber presented a 1-D analytical model of segmented thermoelectric unicouple for operation between 973 and 300 K [11]. In the present paper, we construct a three-dimensional finite element model [12,13] for discussing the performance characteristics of low- and medium-temperature thermoelectric modules. The material properties of the thermoelectric materials such as the Seebeck coefficient, thermal conductivity, and electrical conductivity are temperature dependent. Based on the singe-stage models, we present two- and three-stage models of the solar thermoelectric generator to discuss its performance characteristics. The effect of input energy on performance of solar thermoelectric generator is considered according to the real operating condition.

* Corresponding author at: School of Automotive Engineering, Wuhan University of Technology, Hubei 430070, China.
E-mail addresses: jsxiao@whut.edu.cn (J. Xiao), tqyang@whut.edu.cn (T. Yang), lpwhut@live.whut.edu.cn (P. Li), pczhai@whut.edu.cn (P. Zhai), zhangqj@whut.edu.cn (Q. Zhang).

0306-2619/$ - see front matter © 2011 Elsevier Ltd. All rights reserved.
doi:10.1016/j.apenergy.2011.06.006

Nomenclature

C	specific heat capacity (J/kg K)
T	temperature (°C)
$\dot{q}$	heat generation rate per unit volume (W/m^3)
$\vec{q}$	heat flux vector (W/m^2)
$\vec{J}$	electric current density vector (A/m^2)
$\vec{D}$	electric flux density vector (C/m^2)
$\vec{E}$	electric field intensity vector (V/m)
I	load current (A)
R_L	electric load (Ω)
P	output power (W)
Q_{in}	input power (W)
q_{solar}	solar radiation flux density, 1000 W/m^2
C_g	total concentration ratio of optical focusing system

Greek symbols

ρ	density (kg/m^3)
$[\lambda]$	thermal conductivity matrix (W/mK)
$[\sigma]$	electrical conductivity matrix, S/m
$[\alpha]$	Seebeck coefficient matrix (V/K)
$[\varepsilon]$	dielectric permittivity matrix (F/m)
φ	electric scalar potential (V)
η_{STEG}	total efficiency of solar thermoelectric generator
η_{TE}	thermo electric conversion efficiency
η_{opt}	optical focusing efficiency
η_a	absorptivity of the heat collector

2. Mathematical model of solar thermoelectric generator

2.1. Governing equations of coupled thermoelectricity

The heat flow equation in thermoelectric analysis can be expressed as:

$$\rho C\frac{\partial T}{\partial t}+\nabla\cdot\vec{q}=\dot{q} \tag{1}$$

where ρ, C, T, $\dot{q}$ and $\vec{q}$ stand for density, specific heat capacity, temperature, heat generation rate per unit volume and heat flux vector, respectively.

The continuity equations of electric charge is

$$\nabla\cdot\left(\vec{J}+\frac{\partial\vec{D}}{\partial t}\right)=0 \tag{2}$$

where $\vec{J}$ is the electric current density vector, $\vec{D}$ is the electric flux density vector.

Above two equations are coupled by the set of thermoelectric constitutive equations [12],

$$\vec{q}=T[\alpha]\cdot\vec{J}-[\lambda]\cdot\nabla T \tag{3}$$

$$\vec{J}=[\sigma]\cdot(\vec{E}-[\alpha]\cdot\nabla T) \tag{4}$$

where $[\lambda]$ is the thermal conductivity matrix, $[\sigma]$ is the electrical conductivity matrix, and $[\alpha]$ is the Seebeck coefficient matrix. $\vec{E}=-\nabla\varphi$ is the electric field intensity vector, where φ is the electric scalar potential.

The coupled equations of thermoelectricity can be obtained from above equations,

$$\rho C\frac{\partial T}{\partial t}+\nabla\cdot(T[\alpha]\cdot\vec{J})-\nabla\cdot([\lambda]\cdot\nabla T)=\dot{q} \tag{5}$$

$$\nabla\cdot\left([\varepsilon]\cdot\nabla\frac{\partial\varphi}{\partial t}\right)+\nabla\cdot([\sigma]\cdot[\alpha]\cdot\nabla T)+\nabla\cdot([\sigma]\cdot\nabla\varphi)=0 \tag{6}$$

where $[\varepsilon]$ is the dielectric permittivity matrix.

In the present steady-state model, material properties of all components are considered to be isotropic. The coupled equations of thermoelectricity can be written as follows:

$$\nabla\cdot(T\alpha\vec{J})-\nabla\cdot(\lambda\nabla T)=\dot{q} \tag{7}$$

$$\nabla\cdot(\sigma\alpha\nabla T)+\nabla\cdot(\sigma\nabla\varphi)=0 \tag{8}$$

The equations described in the previous section are solved using the ANSYS which is the commercial software based on the finite element method and is applicable to multiphysics problems [13].

2.2. Model parameters of solar thermoelectric generator

2.2.1. Geometric model

A typical solar thermoelectric generator consists of an optical focusing system, heat collector, thermoelectric module, and cooling plate. The thermoelectric module is the major component of the solar thermoelectric generator. As shown in Fig. 1a, the

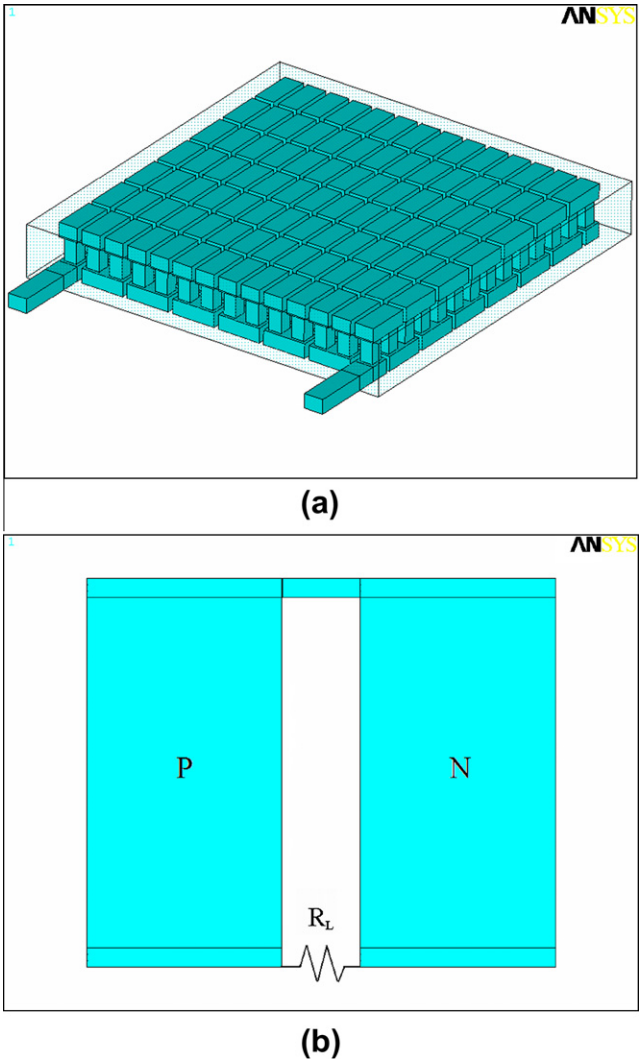

Fig. 1. Geometric model of thermoelectric module and thermoelectric unicouple.

Table 1
Geometric size of thermoelectric unicouple.

Unicouple length (mm)	Unicouple section (mm × mm)	Conductive film thickness (mm)	Unicouple gap (mm)
1.8	1 × 1	0.1	0.4

thermoelectric module consists of conductive film, thermal insulating material and 98 pairs of unicouples. In order to facilitate the calculation, we analyzed only one unicouple in the present paper. The geometric model of the unicouple is shown in Fig. 1b. The p- and n-type thermoelectric materials are connected by the conductive film, and the sawtooth line stand for electric load, the geometric size of the unicouple is shown in Table 1.

2.2.2. Material properties

The selection of thermoelectric materials directly affects the performance of the generator. We used bismuth telluride and filled-skutterudite as materials of the low- and medium-temperature modules, respectively. As the solar thermoelectric generator is operated under large temperature differences, the material properties of the thermoelectric materials such as the Seebeck coefficient, thermal conductivity, and electrical conductivity are temperature dependent [7–9]. The thermal conductivity of the electrically conductive film is 300 W/m K. The contact resistance is not taken into account in the present model.

2.2.3. Boundary conditions

The solar radiation focused by optical focusing system is absorbed by the heat collector for conversion into heat energy. The input heat flux density can be determined as follows [4]:

$$q_{in} = q_{solar} C_g \eta_{opt} \eta_a \tag{9}$$

where q_{solar} is the solar radiation flux density (q_{solar} = 1000 W/m^2) [1,14], C_g is the total concentration ratio of the optical focusing system, η_{opt} is the optical focusing efficiency, and η_a is the absorptivity of the heat collector.

The actual generator is cooled by cooling water. In the present paper, the cooling of generator is assumed to be very good and the first boundary condition is applied to the cold end of the thermoelectric module with a fixed value of 25 °C.

In operation, heat losses mainly include convection loss and radiation loss. Convection heat loss refers to the convection between the surface of the generator and ambient air. Radiation heat loss is the radiation of the surface to ambient. Since the main work of this paper is to study the performance of the solar thermoelectric generator under ideal conditions, the heat losses due to convection and radiation are not taken into account.

2.3. Output power and conversion efficiency of solar thermoelectric generator

The output power is defined as follows,

$$P = I^2 R_L \tag{10}$$

where I and R_L stand for load current and electric load, respectively. So the thermoelectric conversion efficiency can be obtained by,

$$\eta_{TE} = P/Q_{in} \tag{11}$$

where Q_{in} stands for input power. The total efficiency of solar thermoelectric generator is the product of the thermoelectric conversion efficiency η_{TE}, the optical focusing efficiency η_{opt}, and the absorptivity of the heat collector η_a.

$$\eta_{STEG} = \eta_{TE} \eta_{opt} \eta_a \tag{12}$$

3. Results and discussion

3.1. Single-stage thermoelectric modules

The performance of the single-stage thermoelectric modules directly affects the overall solar utilization of solar thermoelectric generator. Therefore, the analysis of generation performances and characteristics for the low- and medium-temperature thermoelectric modules should be carried out prior to the thermal design of the solar thermoelectric generator.

Figs. 2 and 3 show that the conversion efficiency and output power of each module rise with increasing temperature difference. When the temperature difference rises from 0 °C to 200 °C, the conversion efficiency of the bismuth telluride unicouple increases from 0% to 10.82% and the output power from 0 W to 0.0279 W, respectively. Meanwhile, the conversion efficiency and output power of the skutterudite unicouple reaches 9.24% and 0.1009 W, respectively, at the temperature difference of 500 °C. It also can be seen that the performance of the bismuth telluride unicouple is better than that of the skutterudite one when the unicouples are operating between 25 °C and 225 °C. Therefore, effective enhancement of conversion efficiency could be achieved by using multi-stage thermoelectric module which can make full use of the advantages of each thermoelectric material.

3.2. Two-stage thermoelectric module

In above, we analyze the performance of the low- and medium-temperature thermoelectric unicouples. The analysis is the foundation for researching the two-stage thermoelectric module, which consists of a low-temperature module and a medium-temperature module. The medium-temperature module is set at hot end while the low-temperature one is set at cold end in accordance with the optimal work temperature of thermoelectric materials. The simplified model is shown in Fig. 4. The performances of the two-stage thermoelectric unicouple are calculated under different operating conditions.

Figs. 5–7 show that the junction temperature, output power and conversion efficiency of the two-stage thermoelectric unicouple rise with increasing concentration ratio. When the concentration ratio rises to 173, the hot end temperature of the low-temperature thermoelectric unicouple reaches the maximum allowable temperature of bismuth telluride of about 225 °C, and the concentration ratio should not rise any more. Meanwhile, the output power and conversion efficiency of the two-stage unicouple obtains the

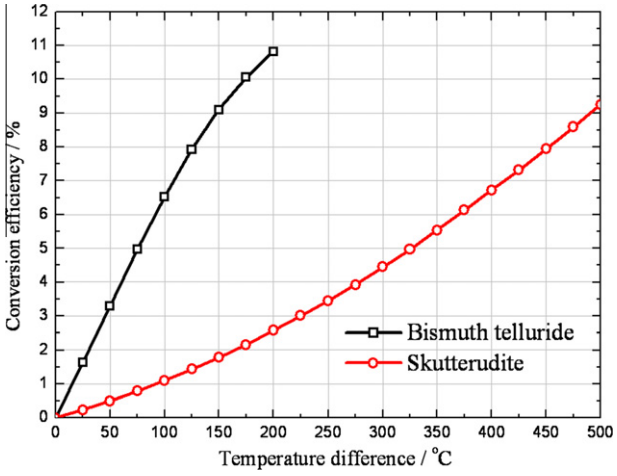

Fig. 2. Dependence of the conversion efficiencies on temperature difference.

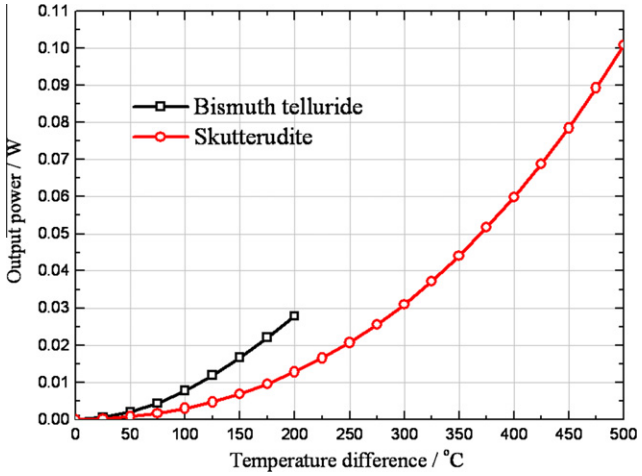

Fig. 3. Dependence of the output power on temperature difference.

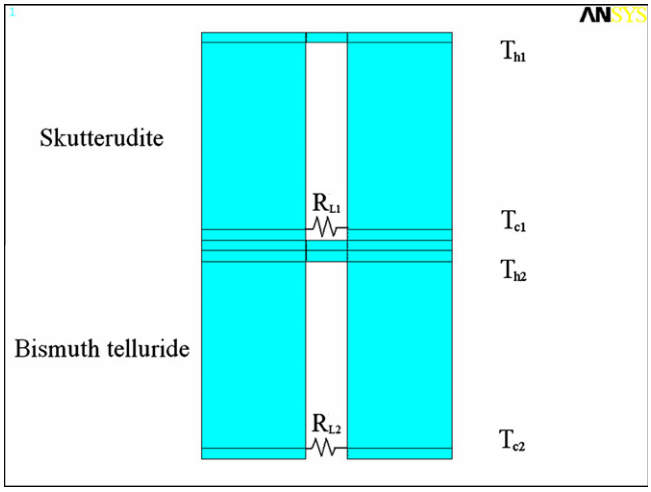

Fig. 4. Geometric model of the two-stage thermoelectric unicouple.

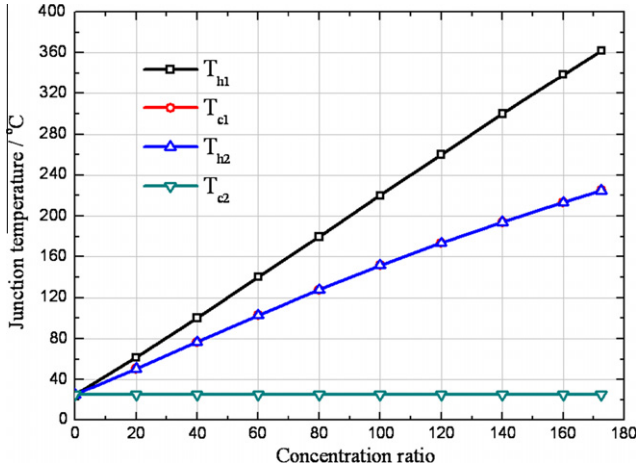

Fig. 5. Dependence of the junction temperature of the two-stage thermoelectric module on concentration ratio.

maximum value of about 0.0353 W and 13.31%, respectively. The contribution of the low-temperature thermoelectric unicouple is about 0.0279 W, while that of the medium-temperature thermoelectric unicouple is about 0.0074 W. It is found that the

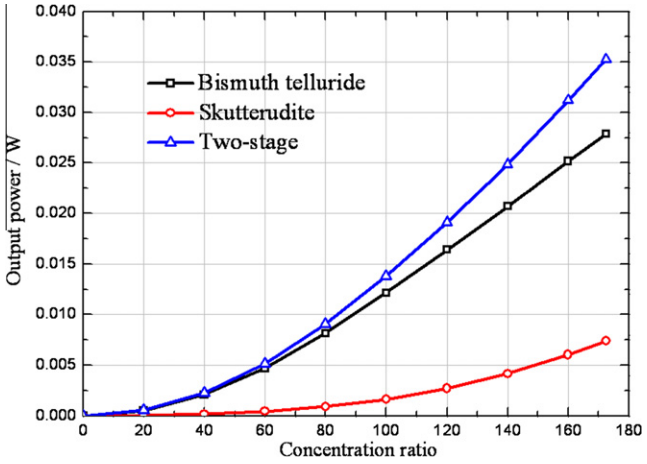

Fig. 6. Dependence of the output power of the two-stage unicouple on concentration ratio.

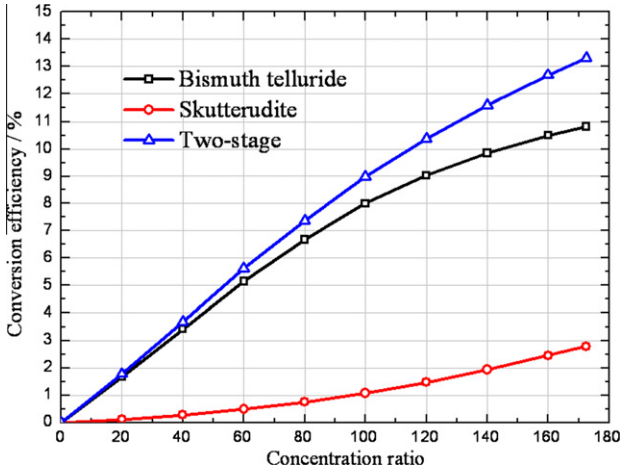

Fig. 7. Dependence of the conversion efficiencies of the two-stage unicouple on concentration ratio.

conversion efficiency of the two-stage module is better than that of the single-stage modules because the thermal-electric conversion occurs twice when the heat energy passing through the two-stage thermoelectric module.

3.3. Three-stage thermoelectric module

It can be seen from the previous analysis of the two-stage module that, when the low-temperature thermoelectric module reaches the maximum allowable temperature of 225 °C, the hot end temperature of the medium-temperature thermoelectric module is 362 °C, far from the maximum allowable temperature of skutterudite of about 525 °C. Therefore, it is feasible to add an extra medium-temperature module on the hot side of the two-stage thermoelectric module to make use of the generating ability of skutterudite between 362 °C and 525 °C. The analysis model of the three-stage thermoelectric module based on one low-temperature module and two medium-temperature modules is established. The simplified model is shown in Fig. 8. Performance analysis under different concentration ratio is carried out.

Fig. 9 shows that when the concentration ratio rises up to 179, the hot end temperature of the low-temperature thermoelectric unicouple reaches the maximum allowable temperature of bismuth telluride (225 °C), while the medium-temperature

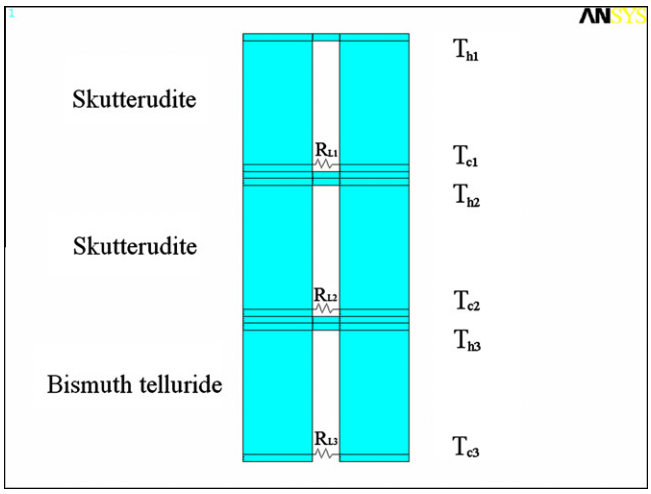

Fig. 8. Geometric model of the three-stage thermoelectric unicouple.

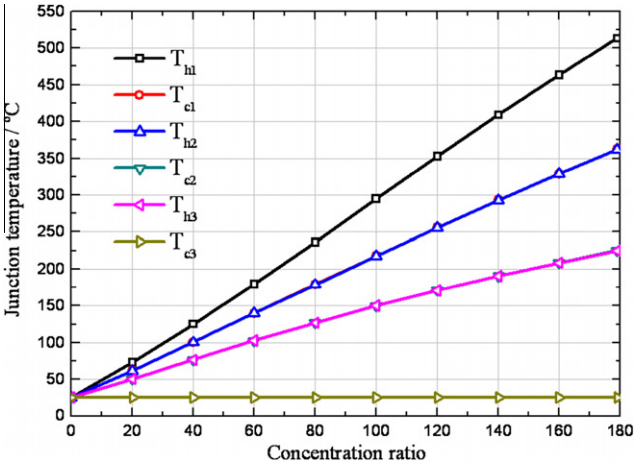

Fig. 9. Dependence of the junction temperature of the three-stage thermoelectric module on concentration ratio.

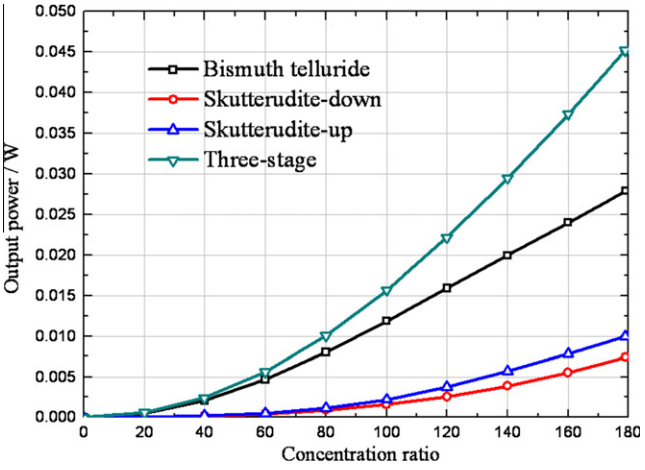

Fig. 10. Dependence of the output power of the three-stage unicouple on concentration ratio.

thermoelectric unicouples is operated between 225 °C and 513 °C approaching to the maximum allowable temperature of skutterudite of about 525 °C.

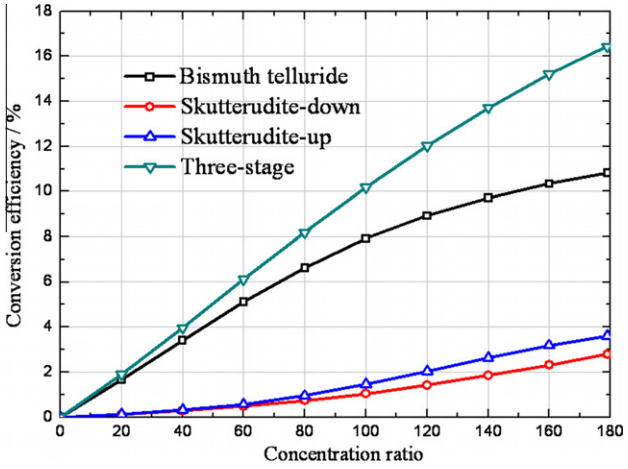

Fig. 11. Dependence of the conversion efficiencies of the three-stage unicouple on concentration ratio.

Table 2
Performance comparison.

Unicouple	Single-stage (Bi_2Te_3)	Two-stage	Three-stage
Concentration ratio	168	173	179
Input power (W)	0.2579	0.2652	0.2749
Output power (W)	0.0279	0.0353	0.0452
Efficiency (%)	10.82	13.31	16.44

Figs. 10 and 11 indicate that the output power and conversion efficiency of the three-stage unicouple obtains the maximum value of 0.0452 W and 16.44%, respectively, at the ultimate concentration ratio. The contribution of the low-temperature thermoelectric unicouple is about 0.0279 W, while that of the two medium-temperature unicouples are 0.0099 W and 0.0074 W, respectively. It can be seen that, the performance of the three-stage unicouple is better than that of the two-stage unicouple (13.31%). The extra medium-temperature module brings an efficiency raise of 3.13%, a relative change of 23.5%. Therefore, the design method of three-stage thermoelectric module can take full advantage of the characteristics of each thermoelectric material and effectively improve the performance of power generation.

3.4. Performance comparison

The optimal performance of the single-stage, two-stage and three-stage unicouples are obtained from above analysis and the comparison of the performances is summarized in Table 2.

It is found that the maximum conversion efficiency of the thermoelectric unicouple gradually increase with increasing stage number. Therefore, high performance of thermoelectric module can be achieved within the large temperature difference by using a multi-stage thermoelectric module. Under a reasonable condition of the efficiency of the optical focusing system $\eta_{opt} = 0.8$ and the absorptivity of the heat collector $\eta_a = 0.8$, if the heat losses and the contact resistance are neglected, the utilization of solar energy of solar thermoelectric generator can reach 10.52%.

4. Conclusion

A 3-D finite element model for thermoelectric module based on low-temperature thermoelectric material bismuth telluride and medium-temperature thermoelectric material filled-skutterudite is established and performance analysis under different operating conditions is carried out. Result shows that, reasonable thermal

design of thermoelectric module can take full advantage of the characteristics of each thermoelectric material and effectively improve the performance of power generation. The total conversion efficiency for solar energy of solar thermoelectric generator based on three-stage thermoelectric module could achieve at 10.52%. With the continuous emergence of new thermoelectric materials, solar thermoelectric generator using multi-stage thermoelectric module will have a good application prospects.

Acknowledgments

This work was supported by the Major Program of National Natural Science Foundation of China (No. 50930004), the National High Technology Research and Development Program of China (863 Program) (No. 2007AA05Z444), and the Major State Basic Research Development Program of China (973 Program) (No. 2007CB607506).

References

[1] Chen JC. Thermodynamic analysis of a solar-driven thermoelectric generator. J Appl Phys 1996;79:2717–21.
[2] Scherrer H, Vikhor L, Lenoir B, Dauscher A, Poinas P. Solar thermoelectric generator based on skutterudites. J Power Sources 2003;115:141–8.
[3] Omer SA, Infield DG. Design optimization of thermoelectric devices for solar power generation. Sol Energy Mater Sol Cells 1998;53:67–82.
[4] Li P, Cai LL, Zhai PC, Tang XF, Zhang QJ, Niino M. Design of a concentration solar thermoelectric generator. J Electron Mater 2010;39:1522–30.
[5] Chen G, Dresselhaus MS, Dresselhaus G, Fleurial JP, Caillat T. Recent developments in thermoelectric materials. Int Mater Rev 2003;48:1–25.
[6] Sootsman JR, Duck YC, Kanatzidis MG. New and old concepts in thermoelectric materials. Angew Chem Int Ed 2009;48:8616–39.
[7] Poudel B, Hao Q, Ma Y, Lan Y, Minnich A, Yu B, et al. High-thermoelectric performance of nanostructured bismuth antimony telluride bulk alloys. Science 2008;320:634.
[8] Zhao XB, Ji XH, Zhang YH, Zhu TJ, Tu JP, Zhang XB. Bismuth telluride nanotubes and the effects on the thermoelectric properties of nanotube-containing nanocomposites. Appl Phys Lett 2005;86:062111.
[9] Tang XF, Zhang QJ, Chen LD, Goto T, Hirai T. Synthesis and thermoelectric properties of p-type- and n-type-filled skutterudite $R_y M_x Co_{4-x} Sb_{12}$ (R: Ce, Ba, Y; M: Fe, Ni). J Appl Phys 2005;97:093712.
[10] Chen LG, Li J, Sun FR, Wu C. Performance optimization of a two-stage semiconductor thermoelectric-generator. Appl Energy 2005;82:300–12.
[11] El-Genk MS, Saber HH. High efficiency segmented thermoelectric unicouple for operation between 973 and 300 K. Energy Convers Manage 2003;44:1069–88.
[12] Antonova EE, Looman DC. Finite elements for thermoelectric device analysis in ANSYS. In: International conference on thermoelectrics. Clemson, US; June 19–23, 2005.
[13] ANSYS Release 10.0 Documentation; 2005.
[14] Kribus A. A high-efficiency triple cycle for solar power generation. Sol Energy 2002;72:1–11.